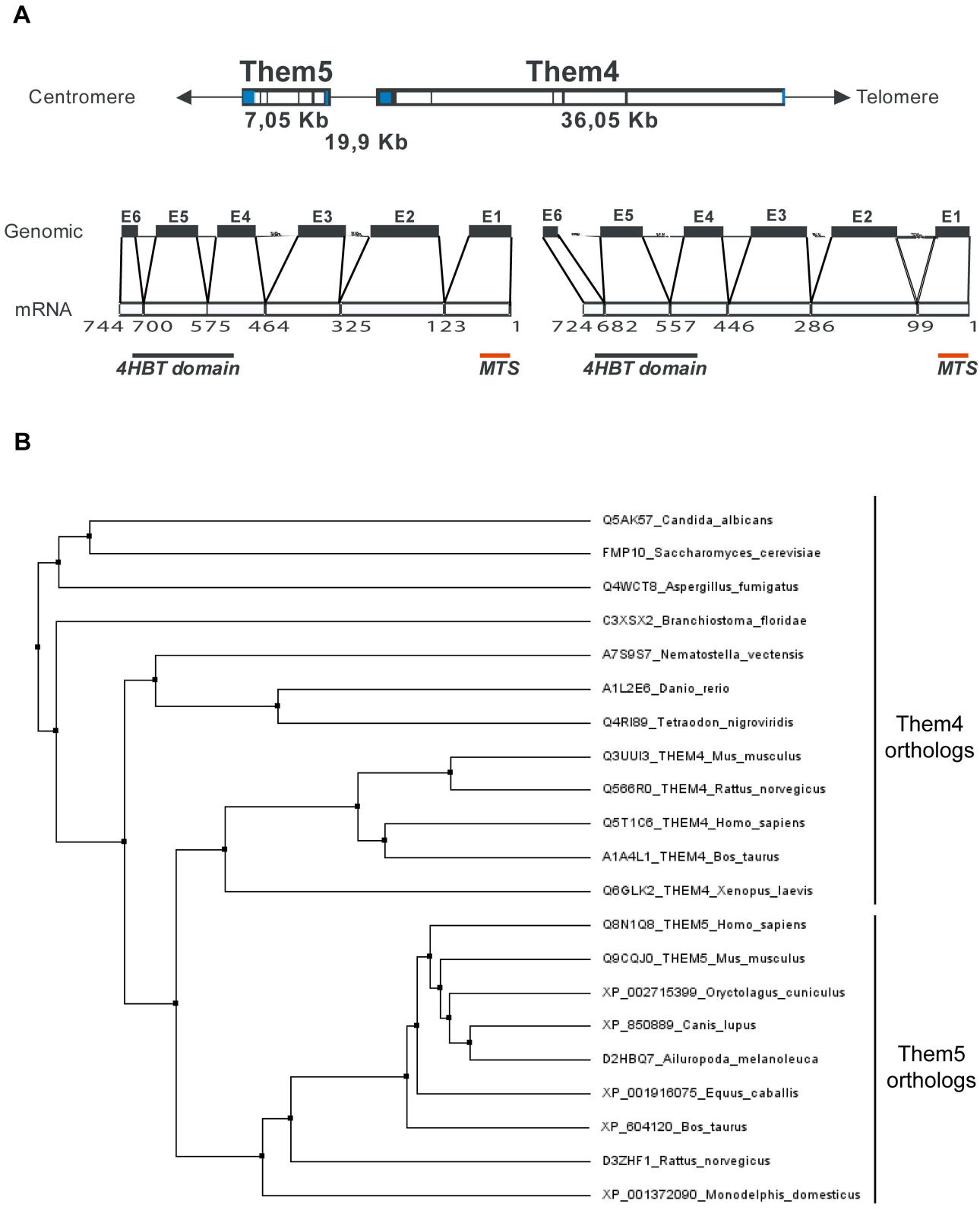
A
Them5
Them4
Centromere
Telomere
7,05 Kb
19,9 Kb
36,05 Kb
Genomic
mRNA
E6
E5
E4
E3
E2
E1
744 700 575 464 325 123 1
724 682 557 446 286 99 1
4HBT domain
MTS
4HBT domain
MTS
B
Q5AK57_Candida_albicans
FMP10_Saccharomyces_cerevisiae
Q4WCT8_Aspergillus_fumigatus
C3XSX2_Branchiostoma_floridae
A7S9S7_Nematostella_vectensis
A1L2E6_Danio_rerio
Q4RI89_Tetraodon_nigroviridis
Q3UUI3_THEM4_Mus_musculus
Q566R0_THEM4_Rattus_norvegicus
Q5T1C6_THEM4_Homo_sapiens
A1A4L1_THEM4_Bos_taurus
Q6GLK2_THEM4_Xenopus_laevis
Q8N1Q8_THEM5_Homo_sapiens
Q9CQJ0_THEM5_Mus_musculus
XP_002715399_Oryctolagus_cuniculus
XP_850889_Canis_lupus
D2HBQ7_Ailuropoda_melanoleuca
XP_001916075_Equus_caballis
XP_604120_Bos_taurus
D3ZHF1_Rattus_norvegicus
XP_001372090_Monodelphis_domesticus
Them4 orthologs
Them5 orthologs

FIG S1. Them5 gene appeared later in evolution but shares similar structure with Them4. (A) Stylized representation of hThem4 and hThem5 genes. Genomic (upper panel) and exon-intron structure and mRNA cartoon representation (lower panel) of hThem4 and hThem5 genes (4HBT - 4-hydroxybenzoyl-CoA thioesterase domain, MTS - mitochondrial targeting sequence). (B) Philogenetic tree of Them4 and Them5 orthologs in different species. Them4 othologs are found in lower eukaryotes, such as yeasts and chordata (Them4 orthologs upper group); Them5 orthologs, however, are present only in mammals (lower group).

A

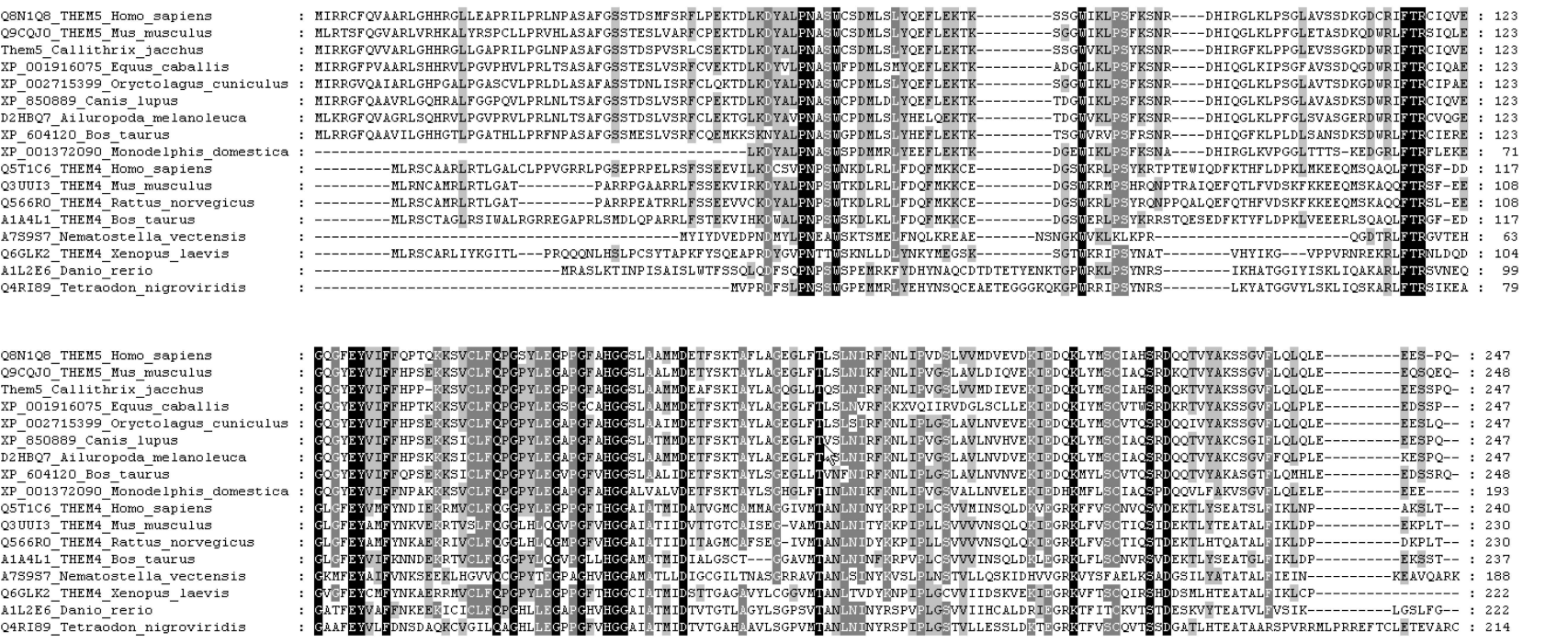
Q8N1Q8_THEM5_Homo_sapiens
Q9CQJ0_THEM5_Mus_musculus
Them5_Callithrix_jacchus
XP_001916075_Equus_caballis
XP_002715399_Oryctolagus_cuniculus
XP_850889_Canis_lupus
D2HBQ7_Ailuropoda_melanoleuca
XP_604120_Bos_taurus
XP_001372090_Monodelphis_domestica
Q5T1C6_THEM4_Homo_sapiens
Q3UUI3_THEM4_Mus_musculus
Q566RO_THEM4_Rattus_norvegicus
A1A4L1_THEM4_Bos_taurus
A7S9S7_Nematostella_vectensis
Q6GLK2_THEM4_Xenopus_laevis
A1L2E6_Danio_rerio
Q4RI89_Tetraodon_nigroviridis

B

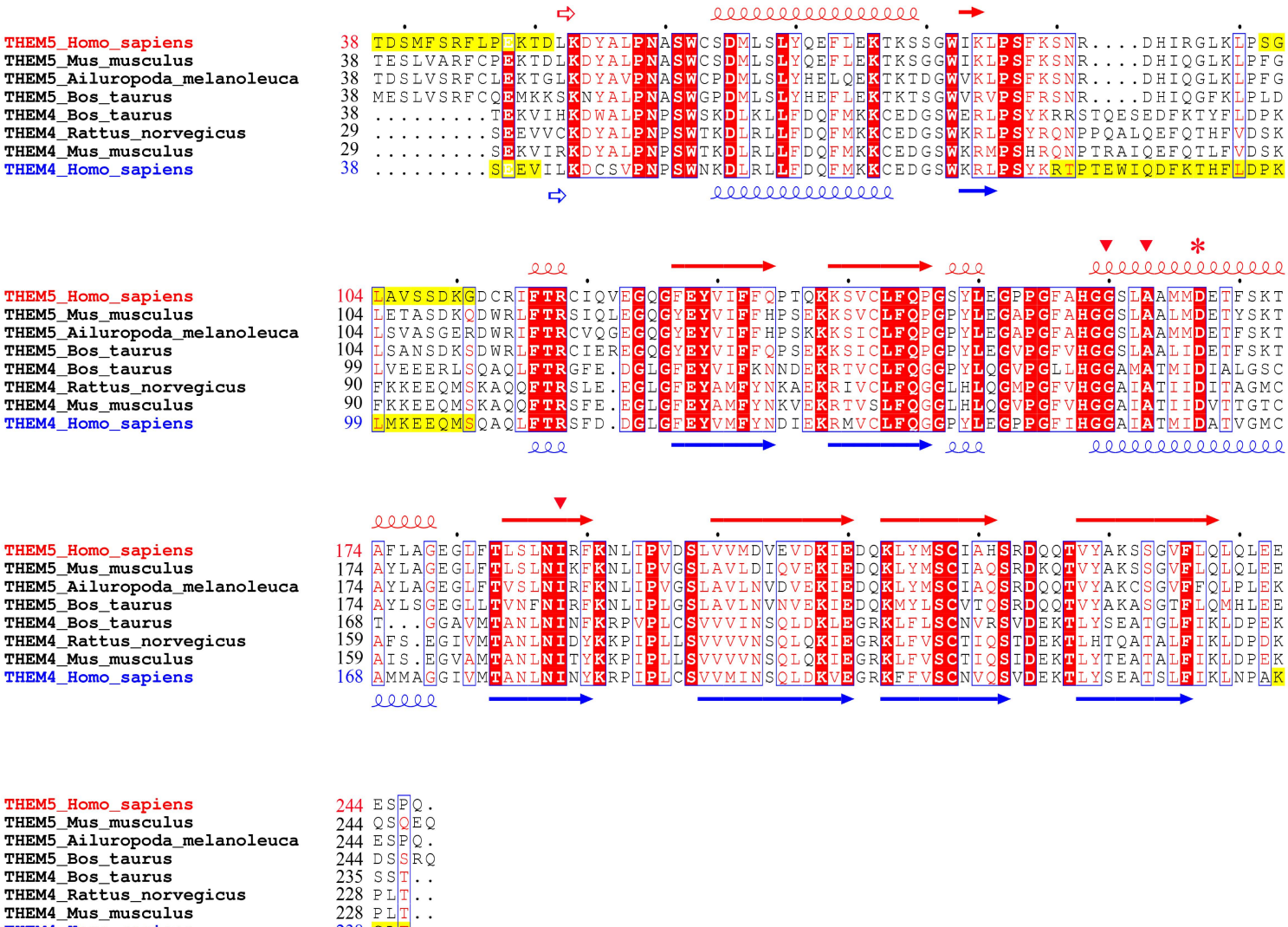
THEM5_Homo_sapiens
THEM5_Mus_musculus
THEM5_Ailuropoda_melanoleuca
THEM5_Bos_taurus
THEM4_Bos_taurus
THEM4_Rattus_norvegicus
THEM4_Mus_musculus
THEM4_Homo_sapiens

C

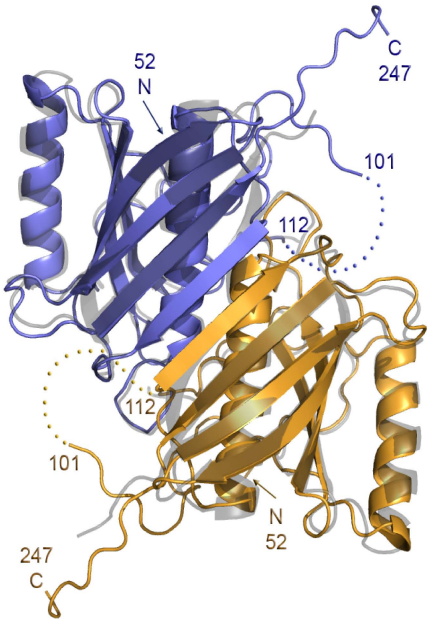

D

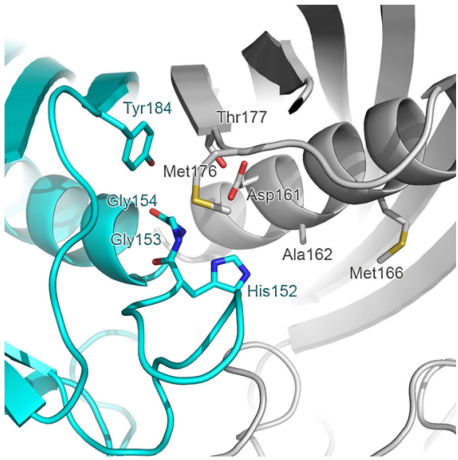

E Steady-state kinetic constants for hThem5 active site mutants

Enzyme		Substrate	K_m (μM)	k_{cat} (s^{-1})	k_{cat}/K_m ($M^{-1}s^{-1}$)
hThem5	T183A	C18:2	0.6	0.2	$3.6x10^5$
hThem5	G160A	C18:2	7.6	0.3	$4.6x10^4$
hThem5	G159A/T183A	C18:2	*n.d.**	0.1	*n.d.*

* - *not possible to determine Km*

FIG S2. Protein sequence and structural analysis of Them4/5 and their orthologs.

(A) ClustalW multiple sequence alignment of Them4/5 and their orthologs in other species used for ConSurf computational analysis (http://consurf.tau.ac.il/). The alignment shows conserved residues (highlighted in dark-grey and grey). Also note the lack of conservation in mitochondrial targeting sequences (N-terminal part of the sequences) between Them4 and Them5 orthologous groups. (B) ClustalW multiple sequence alignment of selected Them5 and Them4 sequences (without predicted MTS). Conserved residues are boxed in red, secondary structure elements in the Δ34Them5 and Δ36Them4 crystal structures are indicated at the top and bottom of the alignment, respectively. The first residues present in the crystallographic models are highlighted with open arrows. Disordered stretches with no electron density, not included in the models, are shown in yellow shading; mutations used in this study are highlighted with red triangles (dimerization) and a red asterisk (enzymatically inactive). (C) Cartoon representation of superimposed crystal structures of Δ34Them5 (blue and orange) and Δ36Them4 (gray, transparent). N- and C-terminal residues in the Δ34Them5 structure are labeled, and disordered stretches not included in the model are shown as dotted lines. (D) Cartoon representation of the putative Δ36Them4 active site. Homodimer subunits are shown in cyan and gray, residues expected to be involved in catalysis and substrate recognition displayed as sticks (atom colors). (E) Steady-state kinetic constants for hThem5 active site mutants in the hydrolysis reaction with linoleyl-CoA, obtained at 37ºC, pH 7.5. T183A mutant displays reduced turnover and k_{cat} (due to the interferes with catalysis), G160A mutant has reduced turnover and k_{cat} (due to the sterical interference in the active site), and G159A/T183A mutant has no activity.

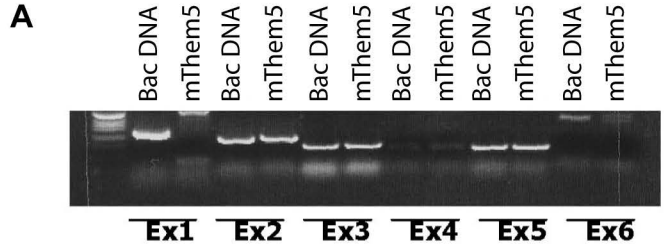
A
Bac DNA
mThem5
Bac DNA
mThem5
Bac DNA
mThem5
Bac DNA
mThem5
Bac DNA
mThem5
Bac DNA
mThem5
Ex1
Ex2
Ex3
Ex4
Ex5
Ex6

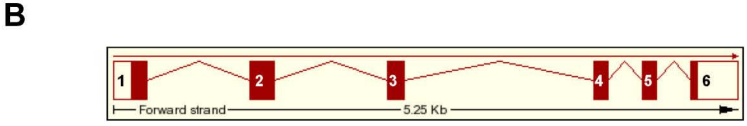
B
1
2
3
4
5
6
Forward strand
5.25 Kb

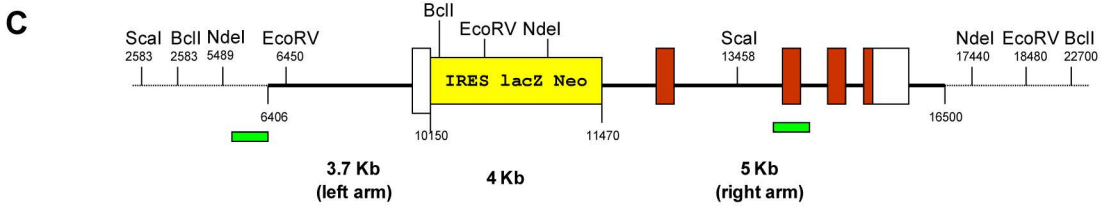
C
ScaI
2583
BclI
2583
NdeI
5489
EcoRV
6450
6406
BclI
EcoRV NdeI
IRES lacZ Neo
10150
11470
ScaI
13458
NdeI
17440
EcoRV
18480
BclI
22700
16500
3.7 Kb
(left arm)
4 Kb
5 Kb
(right arm)

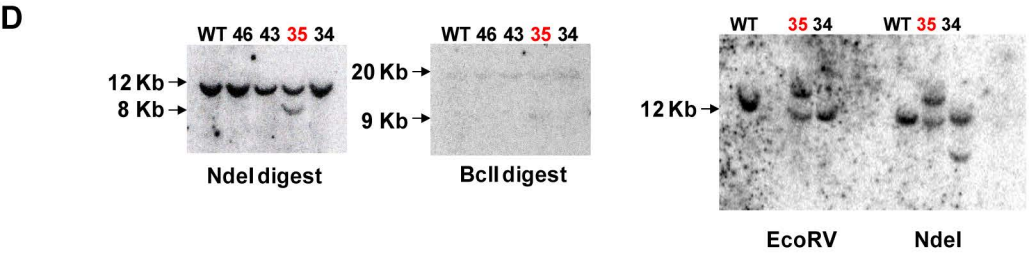
D
WT 46 43 35 34
12 Kb
8 Kb
NdeI digest
WT 46 43 35 34
20 Kb
9 Kb
BclI digest
WT 35 34
WT 35 34
12 Kb
EcoRV
NdeI

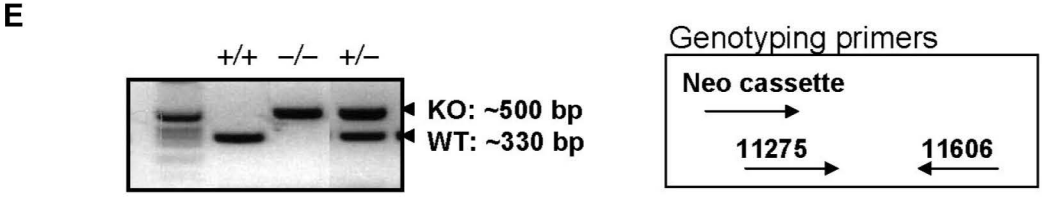
E
+/+
–/–
+/–
KO: ~500 bp
WT: ~330 bp
Genotyping primers
Neo cassette
11275
11606

FIG S3. Generation of Them5 knockout mice. (A) Presence of mThem5 genomic DNA in BAC clone was verified by PCR of individual exons (cloned mThem5 cDNA is positive control). BAC clone was used as PCR template for generating left and right homology region of targeting vector. (B) Transcript structure of mTHEM5 gene in mice. White areas represent untranslated regions (Ensembl database). (C) Targeted *mThem5* allele. A targeting vector was generated that contains a 3.7-kb 5' homology region, an IRES/lacZ/neo cassette, and a 5-kb 3' homology region. A genomic DNA fragment of about 1.3 kb, including the ATG start codon in exon 1 and the full sequence of exon2, is deleted in the targeting vector. The targeting vector was linearized with NotI and electroporated into 129/Ola ES cells. (D) Screening of ES cell clones was performed by Southern blotting. DNA was digested with EcoRV and probed with an external probe (sequence 16980-17663). An internal probe was then used on NdeI digested DNA (sequence 9652-10154) for further characterization of ES cell clones positive for homologous recombination. Correctly targeted ES cells (highlighted in red) were used to generate chimeras. Male chimeras were mated with wild-type C57BL/6 females to obtain *Them5*$^{+/-}$ mice, which were intercrossed to produce *Them5* homozygous mutants. (E) Progeny were genotyped for the presence of a targeted allele by multiplex PCR. The following primers were used for genotyping: P1-as 5'-GCA GCA GGC TGA ACT GAC TGA GG-3'; P2/KO-s 5'- GCT GCC TCG TCC TGC AGT TCA TTC-3''; P3/WT-s 5'-CAG GCG GCT GGA TTA AAC TAC C-3'. One reaction amplifies a 500-bp fragment from the targeted allele and the second reaction amplifies a 330-bp fragment from the wild-type allele.

Figure S4

A

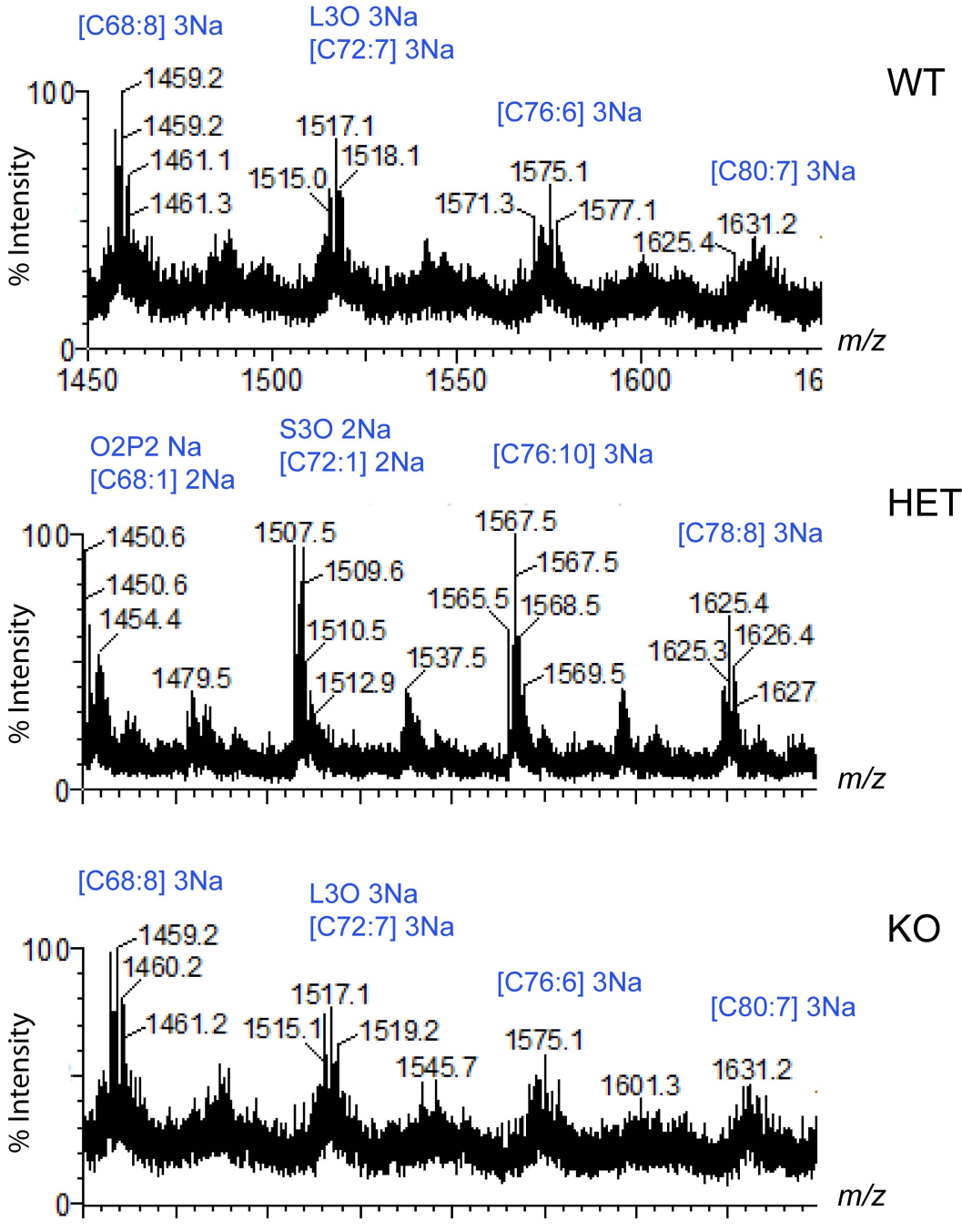
[C68:8] 3Na
L3O 3Na
[C72:7] 3Na
WT
100
1459.2
1459.2
1461.1
1461.3
1515.0
1517.1
1518.1
[C76:6] 3Na
1571.3
1575.1
1577.1
1625.4
[C80:7] 3Na
1631.2
% Intensity
0
m/z
1450
1500
1550
1600
16
O2P2 Na
[C68:1] 2Na
S3O 2Na
[C72:1] 2Na
[C76:10] 3Na
HET
100
1450.6
1450.6
1454.4
1479.5
1507.5
1509.6
1510.5
1512.9
1537.5
1565.5
1567.5
1567.5
1568.5
1569.5
[C78:8] 3Na
1625.3
1625.4
1626.4
1627
% Intensity
0
m/z
[C68:8] 3Na
L3O 3Na
[C72:7] 3Na
KO
100
1459.2
1460.2
1461.2
1515.1
1517.1
1519.2
1545.7
[C76:6] 3Na
1575.1
1601.3
[C80:7] 3Na
1631.2
% Intensity
0
m/z

B

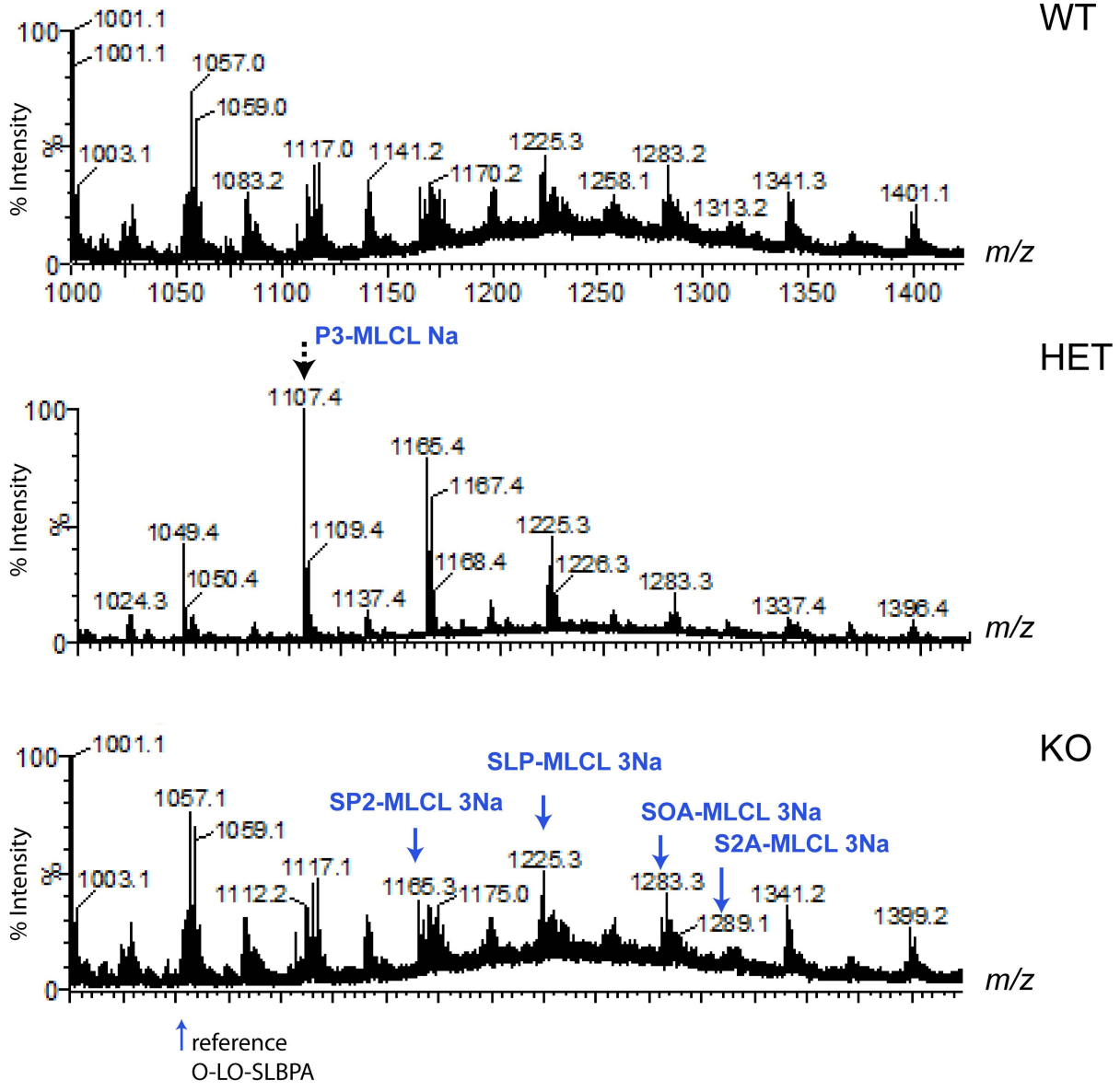
WT
100
% Intensity
0
1001.1
1001.1
1057.0
1059.0
1003.1
1083.2
1117.0
1141.2
1170.2
1225.3
1258.1
1283.2
1313.2
1341.3
1401.1
1000
1050
1100
1150
1200
1250
1300
1350
1400
m/z
HET
P3-MLCL Na
1107.4
1165.4
1167.4
1049.4
1109.4
1225.3
1168.4
1226.3
1050.4
1024.3
1137.4
1283.3
1337.4
1396.4
KO
SLP-MLCL 3Na
SP2-MLCL 3Na
SOA-MLCL 3Na
S2A-MLCL 3Na
1001.1
1057.1
1059.1
1117.1
1003.1
1112.2
1165.3
1175.0
1225.3
1283.3
1289.1
1341.2
1399.2
reference
O-LO-SLBPA

C

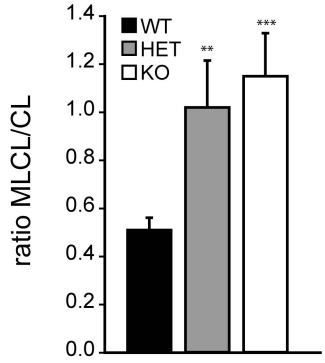
Major MLCL vs major CL
ratio MLCL/CL
WT
HET
KO
**
***
1.4
1.2
1.0
0.8
0.6
0.4
0.2
0.0

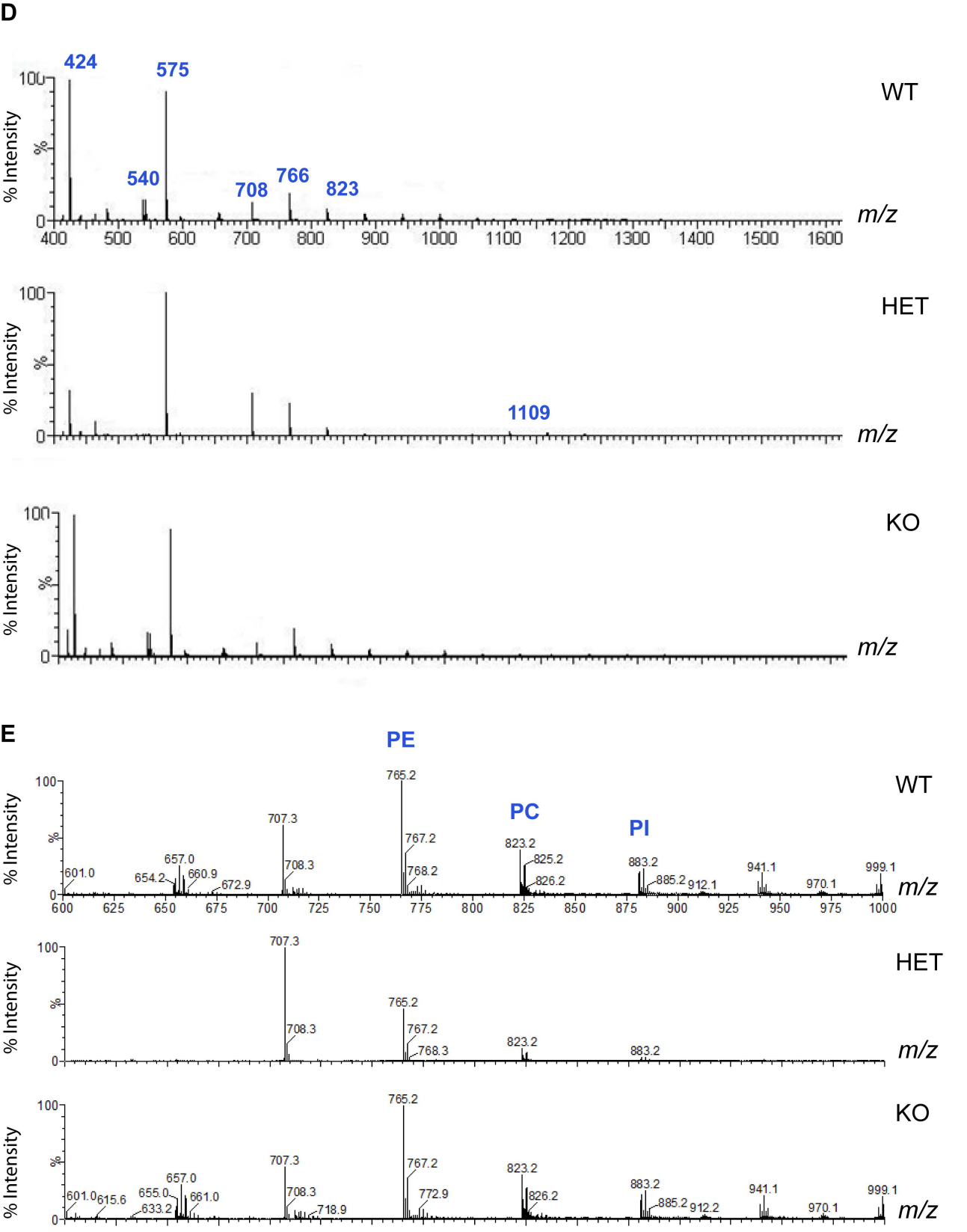
D
424
575
540
708
766
823
WT
% Intensity
m/z
HET
1109
KO
E
PE
PC
PI
765.2
707.3
767.2
823.2
825.2
826.2
883.2
885.2
912.1
941.1
970.1
999.1
601.0
654.2
657.0
660.9
672.9
708.3
768.2
768.3
772.9
615.6
655.0
661.0
633.2
718.9

FIG S4. Mass spectrometry analysis of phospholipid composition. Lipid extracts were prepared from Them5 WT (upper panel), HET (middle) and KO (lower) mouse liver mitochondria and analyzed by mass spectrometry in the positive mode [6]. (A) Detailed species composition in the cardiolipin region, analyzed by MS in the positive mode. The lipid profile shows limited, predominantly quantitative differences in the CL profile between Them5 WT (top panel) and KO (bottom panel) liver mitochondria. P – palmitoyl, S – stearoyl, O – oleoyl, L – lineoyl, A – arachidoyl. (B) Species composition in the MLCL/CL region, as analyzed by MS in positive mode. P – palmitoyl, S – stearoyl, O – oleoyl, L – lineaoyl, A – arachidoyl. (C) Increase in major monolysocardiolipin (MLCL) over cardiolipin (CL) levels upon Them5 ablation. (D) Total spectra analysis of WT and KO samples without major changes between WT and KO. (E) Species composition in the phospholipid region does not show major differences between WT (top) and KO (bottom) samples. Representative MS profiles are shown. PE – phosphatidylethanolamine, PC – phosphatidylcholine, PI – phosphatidylinositol.

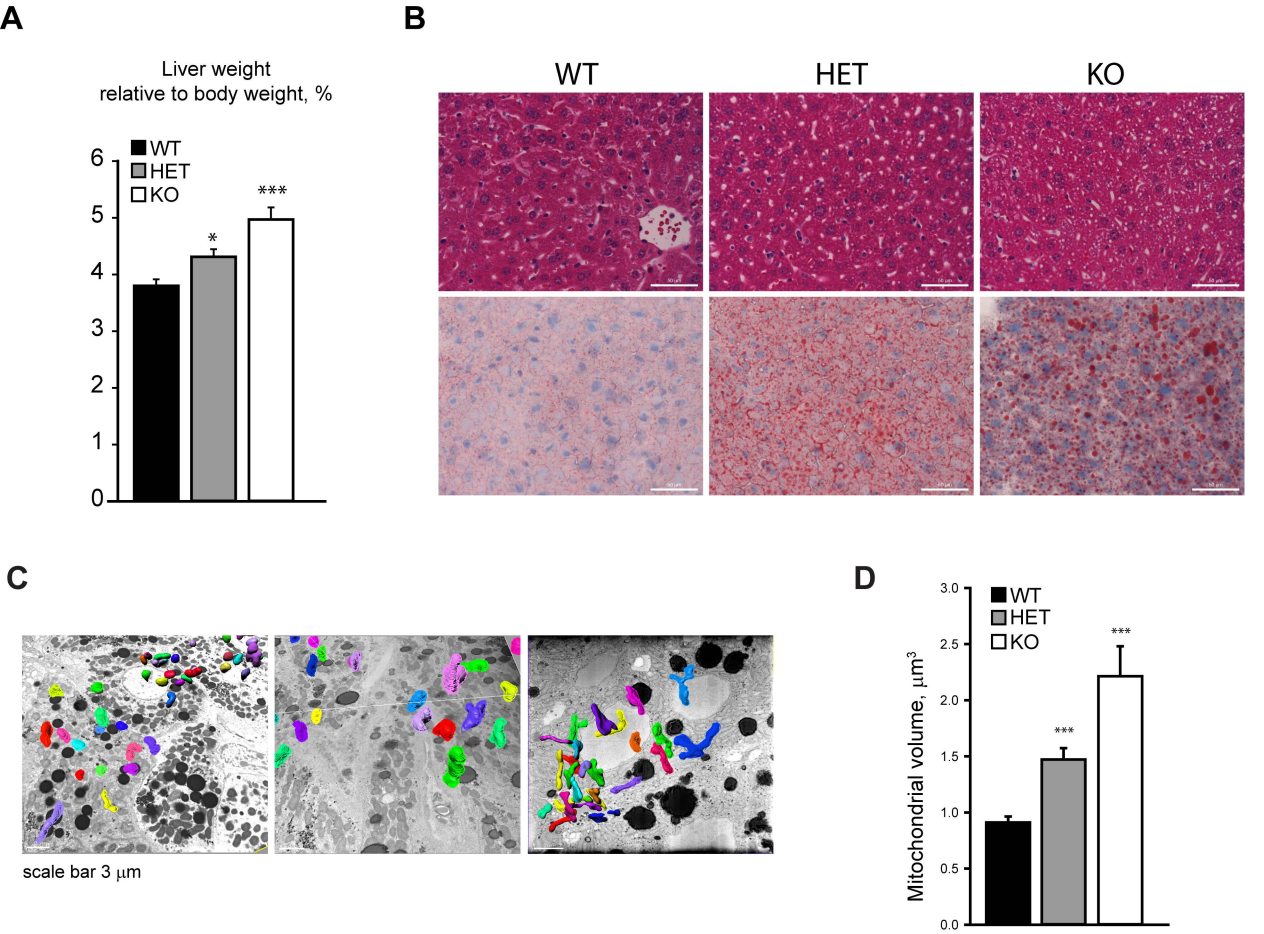
A
Liver weight
relative to body weight, %
WT
HET
KO
*
***
0
1
2
3
4
5
6
B
WT
HET
KO
C
scale bar 3 μm
D
Mitochondrial volume, μm3
WT
HET
KO
***
***
0.0
0.5
1.0
1.5
2.0
2.5
3.0

FIG S5. Loss of Them5 leads to fatty liver development and changes in mitochondria morphology. (A-B) Effect of Them5 loss on fatty liver development, reflected in (A) increased liver weights in Them5 HET and KO mice, as compared to WT littermates (*n*=8-12), and (B) progressive development of liver steatosis in Them5 HET and KO mice. Hematoxylin-eosin staining (top) and Oil Red O staining (bottom) of liver sections from 7-month-old mice (right). (C) Representative electron micrographs of liver cells with 3D reconstructed mitochondria (male mice 3-4 months of age, fasted). (D) Increased mitochondria volume in *Them5*$^{-/-}$ and *Them5*$^{+/-}$ hepatocytes of fasted mice, compared to WT controls (min. 15 mitochondria per cell/mouse were reconstructed, 3 cells/per mouse, *n*=2).